

Evolution of charge density wave order and superconductivity under pressure in LaPt_2Si_2

B. Shen,¹ F. Du,¹ R. Li,¹ A. Thamizhavel,² M. Smidman,¹ Z. Y. Nie,¹ S. S. Luo,¹ T. Le,¹ Z. Hossain,³ and H. Q. Yuan^{1,4,*}

¹*Center for Correlated Matter and Department of Physics, Zhejiang University, Hangzhou 310058, China*

²*DCMP & MS, Tata Institute of Fundamental Research, Mumbai 400005, India*

³*Department of Physics, Indian Institute of Technology, Kanpur 208016, India*

⁴*Collaborative Innovation Center of Advanced Microstructures, Nanjing University, Nanjing, 210093, China*

(Dated: January 15, 2022)

We report measurements of the electrical resistivity and ac magnetic susceptibility of single crystalline LaPt_2Si_2 under pressure, in order to investigate the interplay of superconductivity and CDW order. LaPt_2Si_2 exhibits a first order phase transition from a tetragonal to orthorhombic structure, accompanied by the onset of CDW order below $T_{\text{CDW}} = 76$ K, while superconductivity occurs at a lower temperature of $T_c = 1.87$ K. We find that the application of pressure initially suppresses the CDW transition, but enhances T_c . At pressures above 2.4 GPa, CDW order vanishes, while both T_c and the resistivity A -coefficient reach a maximum value around this pressure. Our results suggest that the occurrence of a superconducting dome can be accounted for within the framework of BCS theory, where there is a maximum in the density of states upon the closure of the CDW gap.

I. INTRODUCTION

The continuous suppression of a phase transition to zero temperature, which is accompanied by superconductivity (SC) in some cases, has long been one of the most intriguing and extensively studied phenomena in condensed matter physics. One recent example is the quantum criticality related to a charge density wave (CDW) phase [1–3]. CDW order corresponds to a condensate with periodic modulations of the electron density, often found in low-dimensional metallic systems. CDW phases have been well documented in various compounds, and in many cases these systems also exhibit superconductivity either in ambient conditions or upon tuning with non-thermal parameters such as pressure [4–9]. Typically, the superconductivity is found to be abruptly enhanced upon suppressing the CDW order [9]. This can be well understood in the framework of Bardeen-Cooper-Schrieffer (BCS) theory, since CDW order gaps out certain regions of the Fermi surface, and as such the suppression of CDW order leads to an enhancement of the superconducting transition temperature T_c due to the sudden enhancement of the density of states at the Fermi level $N(E_F)$.

On the other hand, a different scenario for the interplay of CDW and SC is the occurrence of a superconducting dome on the edge of a CDW/structural instability, as proposed for $T\text{Se}_2$ ($T = \text{Ti}$, and Ta) [1, 2, 10, 11], $\text{Lu}(\text{Pt}_{1-x}\text{Pd}_x)_2\text{In}$ [3], $o\text{-TaS}_3$ [12] and $(\text{Ca},\text{Sr})_3\text{Ir}_4\text{Sn}_{13}$ [13]. SC in conjunction with non-Fermi liquid behaviors is often found in close proximity to a magnetically ordered phase in strongly correlated electronic systems, such as heavy fermion compounds, high T_c cuprates, and iron-based superconductors [14]. In addition, it has been proposed that the accumulation of entropy near a quantum critical point (QCP), due to quantum critical fluctuations, may give rise to novel phases such as supercon-

ductivity [15]. However, one difference between a magnetic QCP in strongly correlated electronic systems and that of a QCP in CDW compounds, is that non-Fermi liquid behaviors seem to be absent in the vicinity of a CDW QCP [1–3]. Furthermore, the observation of CDW domain walls above the superconducting dome and the separation of the CDW QCP and superconductivity in pressurized $1T\text{-TiSe}_2$ seems to challenge the view that the appearance of a superconducting dome is associated with the CDW QCP [16]. Therefore, it is still an open question as to whether critical quantum fluctuations can facilitate SC in the vicinity of a CDW QCP.

LaPt_2Si_2 belongs to the MT_2X_2 ($M = \text{rare earth/alkaline earth}$, $T = \text{transition metal}$, $X = \text{Si or Ge}$) family crystallizing in the CaBe_2Ge_2 -type structure. Several compounds with this structure exhibit both CDW order and SC, such as SrPt_2As_2 [17] and BaPt_2As_2 [18]. SrPt_2As_2 exhibits a CDW transition at around 470 K and becomes superconducting at 5.2 K [17], while BaPt_2As_2 undergoes a first order structural transition at 275 K and a bulk superconducting transition at $T_c = 1.33$ K [18]. Furthermore, BaPt_2As_2 exhibits a complex temperature-pressure phase diagram with multiple pressure-induced transitions at high temperature and abrupt changes in T_c which coincide with the high temperature phase transitions [19].

Studies on polycrystalline LaPt_2Si_2 show that it undergoes a structural phase transition upon cooling, from a tetragonal to orthorhombic phase accompanied by a CDW phase transition at around $T_{\text{CDW}} = 112$ K, and is superconducting below $T_c = 1.8$ K [20]. Meanwhile in single crystals, the CDW order was found at a lower temperature of 80 K [21]. Additional superlattice reflections corresponding to the tripling of the unit cell along the [110] direction [20] strongly suggests the presence of CDW order. Furthermore, CDW order is detected in

other physical quantities such as the thermopower and thermal conductivity [22]. First principles calculations suggest that the Fermi surface of LaPt_2Si_2 is quasi two-dimensional, and that there is coexistence of CDW order and SC in the $[\text{Si}_2\text{-Pt}_1\text{-Si}_2]$ layer [23, 24]. The coexistence of the two orders and a partially opened CDW gap on the Fermi surface were confirmed by nuclear magnetic resonance (NMR) experiments [25]. μSR measurements of LaPt_2Si_2 indicate that the superconductivity is well described by a two-gap s -wave model rather than a single isotropic gap [26]. A pressure study of LaPt_2Si_2 shows the decrease of T_{CDW} and increase of T_c with pressure, but the maximum pressure applied was not high enough to fully suppress the CDW order [27]. It is therefore of great interest to apply higher pressure using a diamond anvil cell so as to investigate the interplay of CDW and SC in LaPt_2Si_2 . Here, we report electrical transport and ac susceptibility measurements of single crystals of LaPt_2Si_2 under pressures up to 7 GPa, and we construct the temperature-pressure phase diagram.

II. EXPERIMENTAL METHODS

Single-crystals of LaPt_2Si_2 were synthesized using the Czochralski method, as described in Ref. [21]. The specific heat down to 0.4 K was measured in a Quantum Design Physical Property Measurement system (PPMS) with a ^3He insert, using a standard pulse relaxation method. The resistivity and ac susceptibility measurements were performed in a Teslatron-PT system with an Oxford ^3He refrigerator, with a temperature range of 0.3 K to 300 K and a maximum applied magnetic field of 8 T. Single crystals of LaPt_2Si_2 were polished and cut into rectangular pieces with approximate dimensions $180\text{ }\mu\text{m} \times 80\text{ }\mu\text{m} \times 30\text{ }\mu\text{m}$, loaded into a BeCu diamond anvil cell (DAC) with a $800\text{-}\mu\text{m}$ -diameter culet. A $100\text{-}\mu\text{m}$ -thick preindented CuBe gasket was covered with Al_2O_3 for electrical insulation and a $400\text{-}\mu\text{m}$ -diameter hole was drilled as the sample chamber. Daphne oil 7373 was used as the pressure-transmitting medium. The DAC was loaded together with several small ruby balls for pressure determination using the ruby fluorescence method at room temperature. For electrical transport measurements, four $15\text{ }\mu\text{m}$ -diameter gold wires were glued to the samples with silver epoxy paste and the resistivity was measured using the standard four-probe method. For ac susceptibility measurements, a 3 Oe magnetic field was generated by the driven coil placed outside the DAC, and two counter wound pickup coils were used to pick up the magnetic signal, with the sample in the center of one of these coils.

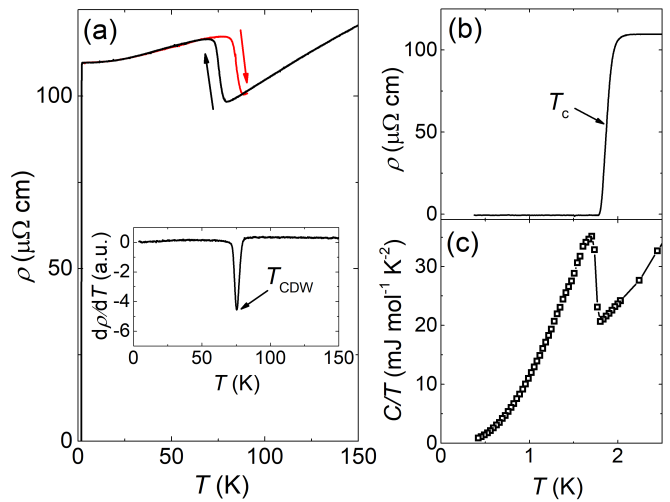


FIG. 1. (color online) (a) Resistivity at ambient pressure of LaPt_2Si_2 as a function of temperature from 150 K down to 0.3 K. The black (red) arrow denotes the data taken upon cooling (warming). (inset) $d\rho/dT$ on cooling which was used to define T_{CDW} . Low temperature (b) resistivity, and (c) specific heat as C/T , which both show the presence of a superconducting transition. The arrow in (b) marks the position of T_c , corresponding to the midpoint of the resistivity drop.

III. RESULTS

Figure 1(a) shows the temperature dependence of the resistivity $\rho(T)$ from 150 K down to 0.3 K at ambient pressure. The resistivity as a function of temperature shows a clear step-like first order phase transition at $T_{\text{CDW}} = 76\text{ K}$, with a hysteresis loop in $\rho(T)$ between measurements performed upon cooling down and warming up. Here T_{CDW} is defined as the minimum of $d\rho/dT$ on the cooling curve, as displayed in the inset of Fig. 1(a). At low temperature, the compound undergoes a superconducting transition at around $T_c = 1.87\text{ K}$, defined as the midpoint of the resistivity drop [Fig. 1(b)]. This also corresponds to the transition observed in the heat capacity $C(T)/T$ [Fig. 1(c)]. Moreover, the sharp nature of the transitions in $\rho(T)$ and $C(T)/T$ indicates a good sample quality. Note that the single crystals of LaPt_2Si_2 studied here show a much lower T_{CDW} but higher T_c than the polycrystalline samples previously reported in Ref. [20]. These differences are likely due to a slight variation in the lattice constants (pressure effect) or sample homogeneity/composition between the polycrystalline and single crystal samples, which might significantly change the values of T_{CDW} and T_c , as shown below.

In order to track the evolution of CDW order, we performed resistivity and ac susceptibility measurements under pressure, where Fig. 2 displays the resistivity of sample No. 1 from 100 K to 1.6 K under various pressures. With the application of pressure, the CDW order is suppressed to lower temperature and the transition becomes broadened. At 2.4 GPa, the CDW transition

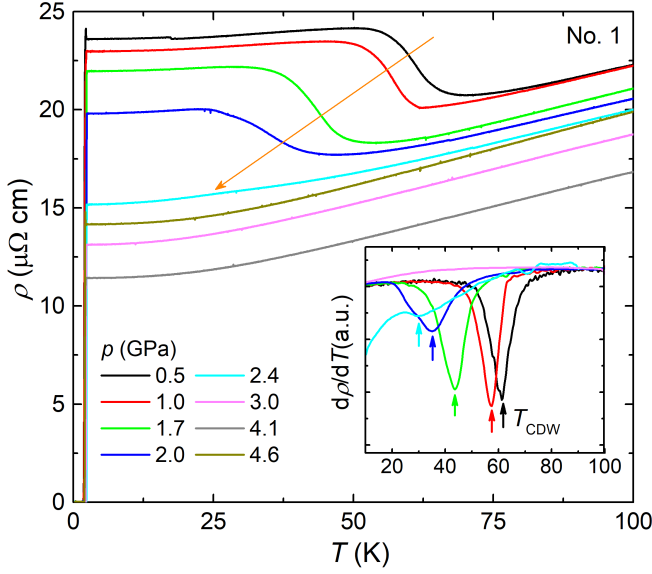


FIG. 2. (color online) Temperature dependence of the resistivity of LaPt₂Si₂ sample No. 1 under various pressures, measured upon cooling. The inset shows the resistivity derivative $d\rho/dT$, where the arrows mark the CDW transition temperatures.

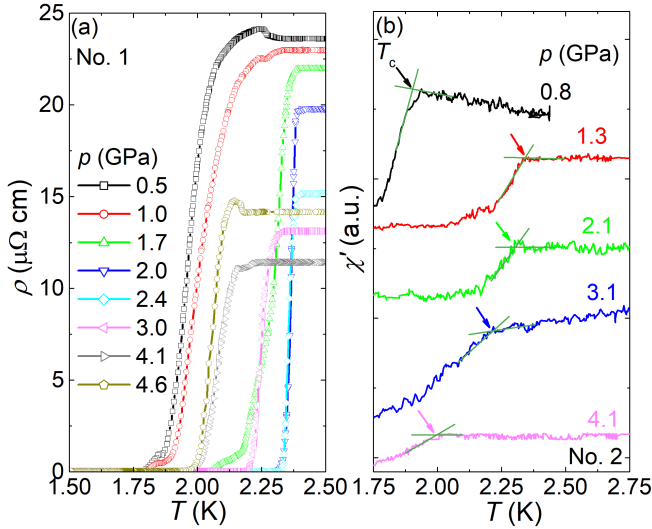


FIG. 3. (color online) Evolution of the superconducting transition of LaPt₂Si₂ under various pressures. The low temperature part of (a) $\rho(T)$ of sample No. 1 and (b) the real part of the ac susceptibility of sample No. 2 are displayed. The arrows in panel (b) indicate the position of T_c .

is hardly seen in the resistivity data, but is still visible in the derivative of the resistivity $d\rho/dT$ as seen in the inset of Fig. 2. With further increasing pressure, there is no signature of the CDW transition in both the resistivity and its derivative. At 3 GPa, $\rho(T)$ shows metallic behavior down to the superconducting transition.

Figure 3(a) displays the low temperature behavior of the resistivity of sample No. 1. Upon applying pressure, T_c initially increases to higher temperatures and reaches

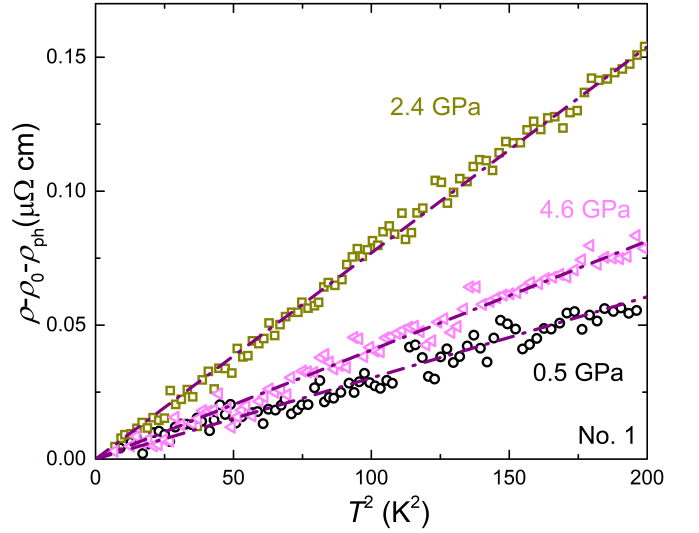


FIG. 4. (color online) Resistivity versus T^2 of sample No. 1 at several pressures, where the residual resistivity ρ_0 and the phonon contribution ρ_{ph} are subtracted. The dashed-dotted lines show the results from fitting Fermi liquid behavior in the normal state.

a maximum value of $T_c^{\max} = 2.36$ K at around 2.0 GPa and 2.4 GPa. The maximum T_c is close to the pressure region where the CDW transition disappears. We also performed ac susceptibility measurements on LaPt₂Si₂ [Fig. 3(b)], from which $T_c(p)$ exhibits similar behavior to the resistivity. Meanwhile, $\rho(T)$ in the normal state of LaPt₂Si₂ under pressure can be fitted using $\rho(T) = \rho_0 + AT^2 + bT^5$, across a wide temperature range. Here, ρ_0 is the residual resistivity, A is the resistivity coefficient related to the Fermi-liquid state, and the last term corresponds to the electron-phonon scattering ρ_{ph} at low temperature. The latter term is valid since the data were fitted at temperatures much lower than the Debye temperature ($\theta_D = 221.3$ K) [21]. The fitted values of b and A are on the order of $10^{-8} \mu\Omega \text{ cm K}^{-5}$ and $10^{-4} \mu\Omega \text{ cm K}^{-2}$ respectively, suggesting that electron-electron scattering dominates the resistivity. Figure 4 displays the resistivity after subtracting ρ_0 and ρ_{ph} as a function of T^2 . The data exhibits a quadratic temperature dependence, indicating a Fermi liquid ground state at all pressures.

From the electrical transport and magnetic susceptibility measurements under pressure, we constructed the temperature-pressure phase diagram of LaPt₂Si₂, which is displayed in Fig. 5(a). As illustrated in the phase diagram, the CDW order shifts to lower temperature with the application of hydrostatic pressure, before suddenly disappearing above around 2.4 GPa. On the other hand, T_c initially increases with pressure, reaching a maximum value at around the pressure where CDW order vanishes. Moreover, the dome-like shape of the superconducting state is different from many other examples of SC competing with CDW order, where T_c often suddenly jumps upon suppressing the CDW transition [9, 28, 29]. Figure

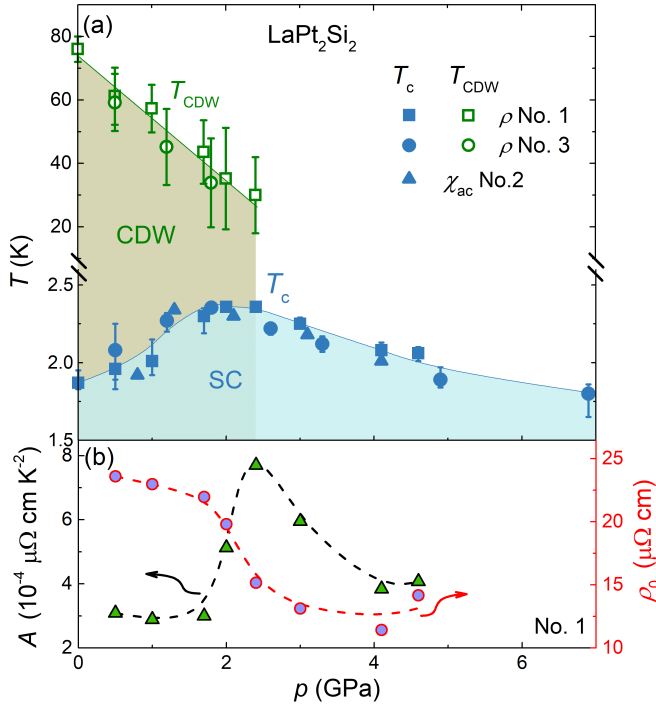


FIG. 5. (color online) (a) Temperature-pressure phase diagram of LaPt₂Si₂. T_{CDW} is determined from the derivative of the resistivity of two samples, where the error bars in T_{CDW} indicate the full width at half minimum of $d\rho/dT$. T_c from $\rho(T)$ corresponds to the temperature where there is a drop to 50 % of the normal state value. For the ac susceptibility, T_c is the temperature of the onset of the transition. The error bars in the T_c from the resistivity represents where there is a 10 % and 90 % drop of the resistivity. (b) Pressure dependence of the A coefficient of the T^2 term in $\rho(T)$ and residual resistivity ρ_0 of sample No. 1.

5(b) shows the results of fitting the resistivity of sample No. 1 where it can be observed that the A coefficient reaches a maximum at around 2.4 GPa, close to the pressure at which the CDW transition abruptly disappears. Furthermore, ρ_0 abruptly decreases upon the suppression of CDW order, which may be related to the closure of the CDW gap.

IV. DISCUSSION

The sudden disappearance of CDW order above 2.4 GPa in LaPt₂Si₂ indicates that there is a first-order transition, suggesting the lack of a QCP, which can account for the absence of non-Fermi liquid behavior across the phase diagram.

As displayed in Fig. 5, both the A -coefficient and T_c have maximum values at around the pressure where CDW order disappears. Since, $A \propto N^2(E_F)$ [30], this suggests that there is a maximum value of $N(E_F)$ at this pressure. Together with the evidence that LaPt₂Si₂ is a conventional electron-phonon mediated superconductor

[21, 26], then a peak in $N(E_F)$ under pressure can lead to a superconducting dome, since $T_c \propto \omega_D \exp[-1/N(E_F)V]$ in BCS theory, where ω_D is a phonon frequency, and V is the electron pairing potential. Note that ω_D and V generally exhibit a more moderate pressure dependence compared to $N(E_F)$ [31]. Therefore, our results suggest that the evolution of T_c under pressure in LaPt₂Si₂ is likely driven by the variation of $N(E_F)$. However, further studies are desirable in order to elucidate the nature of the superconducting state and its pressure evolution.

Below 2.4 GPa, the increase of $N(E_F)$ with increasing pressure can be naturally explained by the suppression of the CDW gap. Above 2.4 GPa, a possible reason for the decrease of $N(E_F)$ is due to band broadening upon compressing the lattice [32, 33]. To confirm this, electronic structure calculations at high pressures are necessary.

It is noted that LaPt₂Ge₂ is also a CDW superconductor, with a lower $T_c = 0.4$ K and a higher $T_{CDW} = 385$ K compared to LaPt₂Si₂. The latter is accompanied by a structural phase transition from the tetragonal CaBe₂Ge₂-type to a monoclinic structure [34, 35]. Moreover, the Fermi surface of LaPt₂Si₂ in the tetragonal phase resembles that of LaPt₂Ge₂ [24, 35]. Upon varying the ratio of Pt and Ge, it was suggested from NMR measurements that enhanced structural fluctuations in LaPt_{2-x}Ge_{2+x} can possibly give rise to the increase of T_c [35]. As such, it would also be of interest to look for the role played by structural fluctuations in influencing the superconductivity of LaPt₂Si₂, which may be addressed by NMR measurements under pressure.

V. CONCLUSION

In conclusion, we have determined the pressure-temperature phase diagram of LaPt₂Si₂, which exhibits both superconductivity and CDW order. With the application of hydrostatic pressure, the CDW order is suppressed to lower temperatures before abruptly vanishing above 2.4 GPa, while T_c shows a dome-like shape with a maximum value at around the same pressure. Furthermore, we suggest that the change of $N(E_F)$ under pressure might account for the SC dome in LaPt₂Si₂ in the framework of BCS theory. Finally, experiments under pressure, such as NMR, and calculations of the electronic structure of LaPt₂Si₂ would be useful to gain further understanding of the interplay between CDW order and superconductivity in this system.

ACKNOWLEDGMENTS

ZH thanks Ritu Gupta for discussion and initial characterization of the sample. This work was supported by the National Key R&D Program of China (Grants No. 2017YFA0303100 and No. 2016YFA0300202), the Na-

tional Natural Science Foundation of China (Grants No. U1632275 and No. 11974306), and the Science Challenge Project of China (Grant No. TZ2016004).

* Corresponding author: hqyuan@zju.edu.cn

- [1] E. Morosan, H. W. Zandbergen, B. S. Dennis, J. W. G. Bos, Y. Onose, T. Klimczuk, A. P. Ramirez, N. P. Ong, and R. J. Cava, “Superconductivity in Cu_xTiSe_2 ,” *Nature Phys.* **2**, 544–550 (2006).
- [2] A. F. Kusmartseva, B. Sipos, H. Berger, L. Forró, and E. Tutiš, “Pressure induced superconductivity in pristine 1T-TiSe_2 ,” *Phys. Rev. Lett.* **103**, 236401 (2009).
- [3] T. Gruner, D. J. Jang, Z. Huesges, R. Cardoso-Gil, G. H. Fecher, M. M. Koza, O. Stockert, A. P. Mackenzie, M. Brandt, and C. Geibel, “Charge density wave quantum critical point with strong enhancement of superconductivity,” *Nature Phys.* **13**, 967–972 (2017).
- [4] L. R. Testardi, “Structural instability and superconductivity in A-15 compounds,” *Rev. Mod. Phys.* **47**, 637–648 (1975).
- [5] L. B. Coleman, M. J. Cohen, D. J. Sandman, F. G. Yamagishi, A. F. Garito, and A. J. Heeger, “Superconducting fluctuations and the peierls instability in an organic solid,” *Solid State Commun.* **12**, 1125 – 1132 (1973).
- [6] J. A. Wilson, F. J. Di Salvo, and S. Mahajan, “Charge-density waves and superlattices in the metallic layered transition metal dichalcogenides,” *Adv. Phys.* **24**, 117–201 (1975).
- [7] H. L. Edwards, A. L. Barr, J. T. Markert, and A. L. de Lozanne, “Modulations in the CuO chain layer of $\text{YBa}_2\text{Cu}_3\text{O}_{7-\delta}$: Charge density waves?” *Phys. Rev. Lett.* **73**, 1154–1157 (1994).
- [8] A. M. Gabovich, A. M. Voitenko, and M. Ausloos, “Charge- and spin-density waves in existing superconductors: competition between cooper pairing and peierls or excitonic instabilities,” *Physics Reports* **367**, 583 – 709 (2002).
- [9] A. M. Gabovich, A. I. Voitenko, J. F. Annett, and M. Ausloos, “Charge- and spin-density-wave superconductors,” *Superconductor Science and Technology* **14**, R1–R27 (2001).
- [10] D. C. Freitas, P. Rodière, M. R. Osorio, E. Navarro-Moratalla, N. M. Nemes, V. G. Tissen, L. Cario, E. Coronado, M. García-Hernández, S. Vieira, M. Núñez-Regueiro, and H. Suderow, “Strong enhancement of superconductivity at high pressures within the charge-density-wave states of 2H-TaS_2 and 2H-TaSe_2 ,” *Phys. Rev. B* **93**, 184512 (2016).
- [11] D. Bhoi, S. Khim, W. Nam, B. S. Lee, C. Kim, B. G. Jeon, B. H. Min, S. Park, and K. H. Kim, “Interplay of charge density wave and multiband superconductivity in $2\text{H-Pd}_x\text{TaSe}_2$,” *Scientific Reports* **6**, 24068 (2016).
- [12] M. Monteverde, J. Lorenzana, P. Monceau, and M. Núñez-Regueiro, “Quantum critical point and superconducting dome in the pressure phase diagram of $\alpha\text{-TaS}_3$,” *Phys. Rev. B* **88**, 180504(R) (2013).
- [13] L. E. Klintberg, S. K. Goh, P. L. Alireza, P. J. Saines, D. A. Tompsett, P. W. Logg, J. H. Yang, B. Chen, K. Yoshimura, and F. M. Grosche, “Pressure- and composition-induced structural quantum phase transition in the cubic superconductor $(\text{Ca}, \text{Sr})_3\text{Ir}_4\text{Sn}_{13}$,” *Phys. Rev. Lett.* **109**, 237008 (2012).
- [14] G. R. Stewart, “Unconventional superconductivity,” *Advances in Physics* **66**, 75–196 (2017).
- [15] K. Grube, S. Zaum, O. Stockert, and Q. Si, “Multi-dimensional entropy landscape of quantum criticality,” *Nature Phys.* **13**, 742–745 (2017).
- [16] Y. I. Joe, X. M. Chen, P. Ghaemi, K. D. Finkelstein, G. A. de la Pea, Y. Gan, J. C. T. Lee, S. Yuan, J. Geck, G. J. MacDougall, T. C. Chiang, S. L. Cooper, E. Fradkin, and P. Abbamonte, “Emergence of charge density wave domain walls above the superconducting dome in 1T-TiSe_2 ,” *Nature Phys.* **10**, 421–425 (2014).
- [17] A. F. Fang, T. Dong, H. P. Wang, Z. G. Chen, B. Cheng, Y. G. Shi, P. Zheng, G. Xu, L. Wang, J. Q. Li, and N. L. Wang, “Single-crystal growth and optical conductivity of SrPt_2As_2 superconductors,” *Phys. Rev. B* **85**, 184520 (2012).
- [18] W. B. Jiang, C. Y. Guo, Z. F. Weng, Y. F. Wang, Y. H. Chen, Y. Chen, G. M. Pang, T. Shang, T. Lu, and H. Q. Yuan, “Superconductivity and structural distortion in BaPt_2As_2 ,” *J. Phys.: Condens. Matter* **27**, 022202 (2014).
- [19] C. Y. Guo, W. B. Jiang, M. Smidman, F. Han, C. D. Malliakas, B. Shen, Y. F. Wang, Y. Chen, X. Lu, M. G. Kanatzidis, and H. Q. Yuan, “Superconductivity and multiple pressure-induced phases in BaPt_2As_2 ,” *Phys. Rev. B* **94**, 184506 (2016).
- [20] Y. Nagano, N. Araoka, A. Mitsuda, H. Yayama, H. Wada, M. Ichihara, Ma. Isobe, and Y. Ueda, “Charge density wave and superconductivity of LaPt_2Si_2 ($\text{R} = \text{Y}, \text{La}, \text{Nd}$, and Lu),” *J. Phys. Soc. Jpn.* **82**, 064715 (2013).
- [21] R. Gupta, S. K. Dhar, A. Thamizhavel, K. P. Rajeev, and Z. Hossain, “Superconducting and charge density wave transition in single crystalline LaPt_2Si_2 ,” *J. Phys.: Condens. Matter* **29**, 255601 (2017).
- [22] R. Gupta, K. P. Rajeev, and Z. Hossain, “Thermal transport studies on charge density wave materials LaPt_2Si_2 and PrPt_2Si_2 ,” *J. Phys.: Condens. Matter* **30**, 475603 (2018).
- [23] I. Hase and T. Yanagisawa, “Electronic structure of LaPt_2Si_2 ,” *Physica C: Superconductivity* **484**, 59 – 61 (2013).
- [24] S. Kim, K. Kim, and B. I. Min, “The mechanism of charge density wave in Pt-based layered superconductors: SrPt_2As_2 and LaPt_2Si_2 ,” *Sci. Rep.* **5**, 15052 (2015).
- [25] T. Aoyama, T. Kubo, H. Matsuno, H. Kotegawa, H. Tou, A. Mitsuda, Yu. Nagano, N. Araoka, H. Wada, and Y. Yamada, “ ^{195}Pt -NMR evidence for opening of partial charge-density-wave gap in layered LaPt_2Si_2 with CaBe_2Ge_2 structure,” *J. Phys. Soc. Jpn.* **87**, 124713 (2018).
- [26] D. Das, R. Gupta, A. Bhattacharyya, P. K. Biswas, D. T. Adroja, and Z. Hossain, “Multigap superconductivity in the charge density wave superconductor LaPt_2Si_2 ,” *Phys. Rev. B* **97**, 184509 (2018).
- [27] R. Gupta, A. Thamizhavel, P. Rodière, S. Nandi, K. P. Rajeev, and Z. Hossain, “Electrical resistivity under pressure and thermal expansion of LaPt_2Si_2 single crystal,” *Journal of Applied Physics* **125**, 143902 (2019).
- [28] O. Degtyareva, M. V. Magnitskaya, J. Kohanoff, G. Profeta, S. Scandolo, M. Hanfand, M. I. McMahon, and E. Gregoryanz, “Competition of charge-density waves and superconductivity in sulfur,” *Phys. Rev. Lett.* **99**,

- 155505 (2007).
- [29] X. D. Zhu, W. Ning, L. J. Li, L. S. Ling, R. R. Zhang, J. L. Zhang, K. F. Wang, Y. Liu, L. Pi, Y. C. Ma, H. F. Du, M. L. Tian, Y. P. Sun, C. Petrovic, and Y. H. Zhang, “Superconductivity and charge density wave in $\text{ZrTe}_{3-x}\text{Se}_3$,” *Scientific Reports* **6**, 26974 (2016).
 - [30] M. J. Rice, “Electron-electron scattering in transition metals,” *Phys. Rev. Lett.* **20**, 1439–1441 (1968).
 - [31] M. Núñez Regueiro, J. M. Mignot, and D. Castello, “Superconductivity at high pressure in NbSe_3 ,” *EPL (Europhysics Letters)* **18**, 53 (1992).
 - [32] J. J. Hamlin, “Superconductivity in the metallic elements at high pressures,” *Physica C: Superconductivity and its Applications* **514**, 59–76 (2015).
 - [33] M. Monteverde, M. Nunez-Regueiro, N. Rogado, K. A. Regan, M. A. Hayward, T. He, S. M. Loureiro, and R. J. Cava, “Pressure dependence of the superconducting transition temperature of magnesium diboride,” *Science* **292**, 75–77 (2001).
 - [34] G. W. Hull, J. H. Wernick, T. H. Geballe, J. V. Waszczak, and J. E. Bernardini, “Superconductivity in the ternary intermetallics YbPd_2Ge_2 , LaPd_2Ge_2 , and LaPt_2Ge_2 ,” *Phys. Rev. B* **24**, 6715–6718 (1981).
 - [35] S. Maeda, K. Matano, R. Yatagai, T. Oguchi, and G. Q. Zheng, “Superconductivity and the electronic phase diagram of $\text{LaPt}_{2-x}\text{Ge}_{2+x}$,” *Phys. Rev. B* **91**, 174516 (2015).